

A Compact Dual-Band CPW-Fed Planar Monopole Antenna for 2.62-2.73 GHz Frequency Band, WiMAX and WLAN Applications

Ahmed Zakaria Manouare¹, Saida Ibnyaich², Abdelaziz EL Idrissi¹, Abdelilah Ghammaz¹

¹Department of Applied Physics, Laboratory of Electrical Systems and Telecommunications, Faculty of Sciences and Technologies, Cadi Ayyad University, Marrakesh, Morocco.

²Department of Physics, Laboratory of Electronics and Instrumentation, Faculty of Sciences Semlalia, Cadi Ayyad University, Marrakesh, Morocco.
ahmedzakaria.manouare@gmail.com

Naima Amar Touhami³

³Laboratory of Information Systems and Telecommunications, Faculty of Sciences, Abdelmalek Essaadi University, Tetouan, Morocco.

Abstract— In this paper, we present a compact and low-profile monopole antenna with a simple structure for the 2.6-2.73 GHz frequency band, the Worldwide Interoperability for Microwave Access (WiMAX) and the Wireless Local Area Network (WLAN) applications. The first configuration of our antenna mainly consists by three radiating elements: inverted L-shaped Stub1, L-shaped Stub2 and a rectangle Stub3. By adjusting the lengths of the three Stubs, three resonant frequencies can be achieved and adjusted separately. Then, the assembled between Stub2 and Stub3 gives the final design of our proposed antenna with a small overall size of 20 mm × 37 mm × 1.56 mm. From the experimental results it is observed that, the antenna prototype has achieved two operating bandwidths ($S_{11} \leq -10$ dB): the first band from 2.62 to 2.73 GHz (110 MHz) and a second broadband from 3.02 to 7.30 GHz (4280 MHz) which combines WiMAX and WLAN applications. The antenna also exhibits an almost omnidirectional radiation patterns over the operating bands. The parameters which affect the performance of the antenna in terms of its frequency domain characteristics are studied in this paper. The details of the monopole antenna design along with simulated and experimental results are presented and discussed.

Index Terms— CPW-feed, Dual-band antenna, Monopole antenna, Multiband antenna, WiMAX/WLAN applications.

I. INTRODUCTION

In modern wireless communication systems, multiband antenna has been playing a very important role for wireless service requirements. Wireless Local Area Network (WLAN) and Worldwide Interoperability for Microwave Access (WiMAX) have been widely applied to mobile devices such as handheld computers and smart phones, more and more engineers and researchers have focused their interests on how to design multiband antennas that can be integrated in a portable wireless communication device for several communication standards. In order to satisfy the IEEE 802.11

WLAN standards in the 5.2 GHz (5150–5350 MHz)/5.8 GHz (5725–5825 MHz) operating bands and WiMAX 2.6/3.5/5.5 GHz (2500–2690/3400–3690/5250–5850 MHz) bands, multi-band antennas with low cost, compact size, easy fabrication and higher performance are required. Several dual-band antennas for WLAN applications were presented [1-5]. To enhance the bandwidth, a dual wideband monopole antenna was realized with a parasitic patch using electromagnetic coupling mechanism to cover the whole WLAN bands and WiMAX bands. However, the overall size of the antenna is somewhat large ($48 \times 58 \text{ mm}^2$), occupying much of the device space [6]. A compact wideband L-shaped monopole antenna with enough bandwidth to cover the whole WLAN and WiMAX operating bands was obtained in [7]. A compact dual-wideband antenna with assembled monopoles is proposed in [8]. A coplanar waveguide (CPW)-fed printed monopole antenna with an n-shaped slot for dual-band operation is presented in [9]. In [10], a dual-band slotted patch antenna with defective ground has been designed to cover WLAN and WiMAX applications. In reference [11], a CPW-fed compact meandered patch antenna for dual-band operation is presented. In [12], a CPW-fed dual-frequency monopole antenna has been reported. In [13], a square-slot antenna with symmetrical L-strips is presented for WLAN and WiMAX applications, but the three resonant frequencies cannot be tuned independently. Many promising UWB antennas have been discussed in the literature [14-18].

In this paper, we present a compact dual-band CPW-fed planar monopole antenna for 2.6-2.73 GHz frequency band, WiMAX and WLAN applications. The first stage of our design is a simple antenna with three Stubs (Stub1, Stub2 and Stub3) which provides three resonant frequencies at 2.603 GHz, 3.429 GHz and 4.584 GHz. These frequencies can be tuned individually according to the parameters L_1 , L_2 and L_3 , as shown in Fig. 1 (a). In the second stage, by assembling the Stub2 and the Stub3, as shown in Fig. 1 (b), the proposed antenna satisfies a part of the 2.6 GHz band (first band) from 2.62 to 2.73 GHz and a second wide band from 3.02 to 7.30 GHz is formed to cover all the 5.2/5.8 GHz WLAN operating bands and the 3.5/5.5 GHz WiMAX operating bands. Details of the antenna design and the effects of the key structure parameters on the antenna performances are neatly examined and discussed.

II. ANTENNA DESIGN

The geometries of the initial and proposed CPW-fed monopole antennas are shown in Fig. 1. Both the antennas are designed on a 1.56 mm thick FR4 substrate having relative permittivity of 4.3, a loss tangent of 0.025 and having overall dimensions of $20 \text{ (W)} \times 37 \text{ (L)} \text{ mm}^2$ and a coppering thickness of the radiator $t = 0.035 \text{ mm}$. The electromagnetic simulation software CST Microwave Studio based on Finite Integration Technique (FIT) is used for the design. In both antennas, the CPW has a feed width of $W_f = 2.8 \text{ mm}$ and a gap distance of $g = 0.4 \text{ mm}$ between the feed and the coplanar ground plane, which corresponds to 50Ω characteristic impedance.

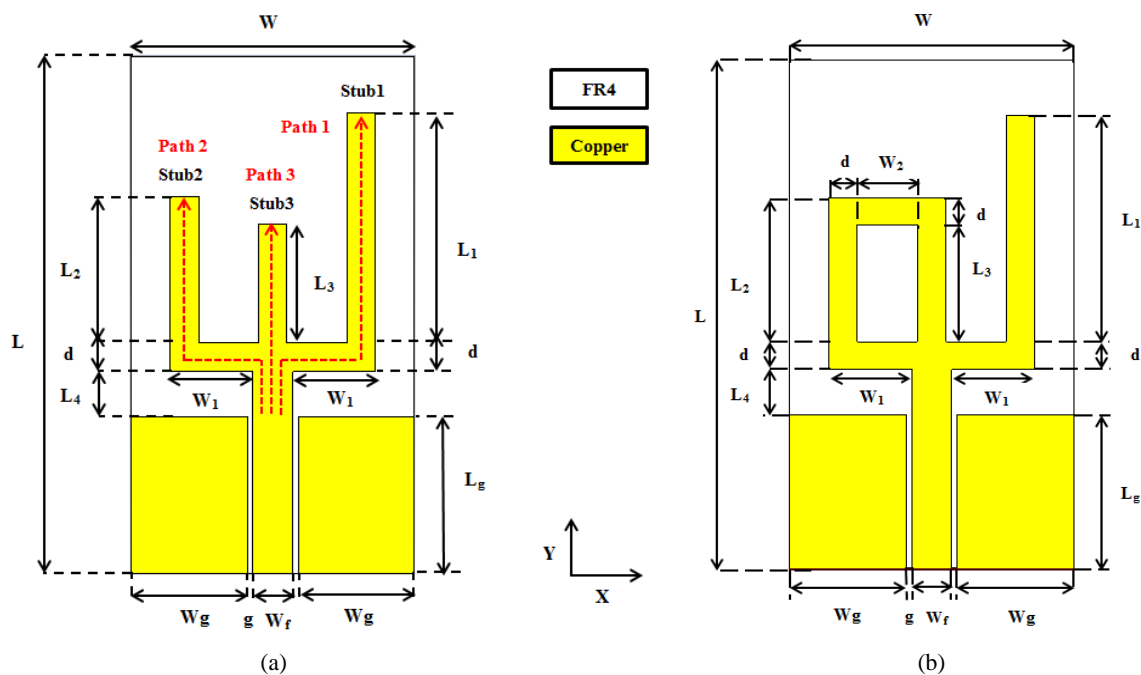


Fig. 1. (a) Geometry of the initial antenna, (b) Geometry of the proposed antenna.

The radiating element is composed by three Stubs: inverted L-shaped Stub1 with $L_1 = 16.5$ mm, L-shaped Stub2 with $L_2 = 10.5$ mm and a rectangle Stub3 with $L_3 = 8.5$ mm, as shown in Fig. 1 (a). By adjusting the lengths (L_1 , L_2 and L_3) of these Stubs, three resonant frequencies can be generated and adjusted independently. The optimized geometrical parameters describing the proposed antenna are tabulated in Table I.

TABLE I. THE OPTIMIZED PROPOSED ANTENNA PARAMETERS

Parameters	Values (mm)
W	20
L_1	16.5
L_3	8.5
W_1	7.225
L_g	11.2
d	2
L	37
L_2	10.5
L_4	3.3
W_g	8.2
W_f	2.8
W_2	5.625

Fig. 2 shows the different shapes in the evolution of the proposed antenna and the simulated result of the reflection coefficient of the proposed antenna is presented in Fig. 3. The structure illustrated in Shape 1 of Fig. 2 is the basic CPW-fed planar antenna which consists by an inverted L-shaped Stub1 acting as the monopole. When an additional L-shaped Stub2 is embedded to the monopole of Shape 1 (Shape 2), a second resonant mode at 3.50 GHz band is generated and two operating bandwidths are

obtained. Afterwards, a rectangle Stub3 is added to the Shape 2 (Shape 3) and the triple-band structure is obtained: The first band from 2.519 to 2.673 GHz (154 MHz) centered at 2.603 GHz, the second band from 3.058 to 4 GHz (942 MHz) centered at 3.429 GHz and the third band from 4.437 to 6.761 GHz (2324 MHz) centered at 4.584 GHz.

Finally, we can observe that the assembled between Stub2 and Stub3 (Proposed antenna) can provide a wide band which cover all the WiMAX 3.5/5.5 GHz bands and the WLAN 5.2/5.8 GHz bands. From the simulated reflection coefficient of this proposed monopole antenna, a resonance at about 2.65 GHz is seen for the first band and two resonance frequencies 3.50 GHz and 5.956 GHz are showed for the second broadband. Two operating bandwidths ($S_{11} \leq -10$ dB) are achieved: The first band from 2.519 to 2.729 GHz (210 MHz) and the second band from 3.093 to 6.684 GHz (3591 MHz).

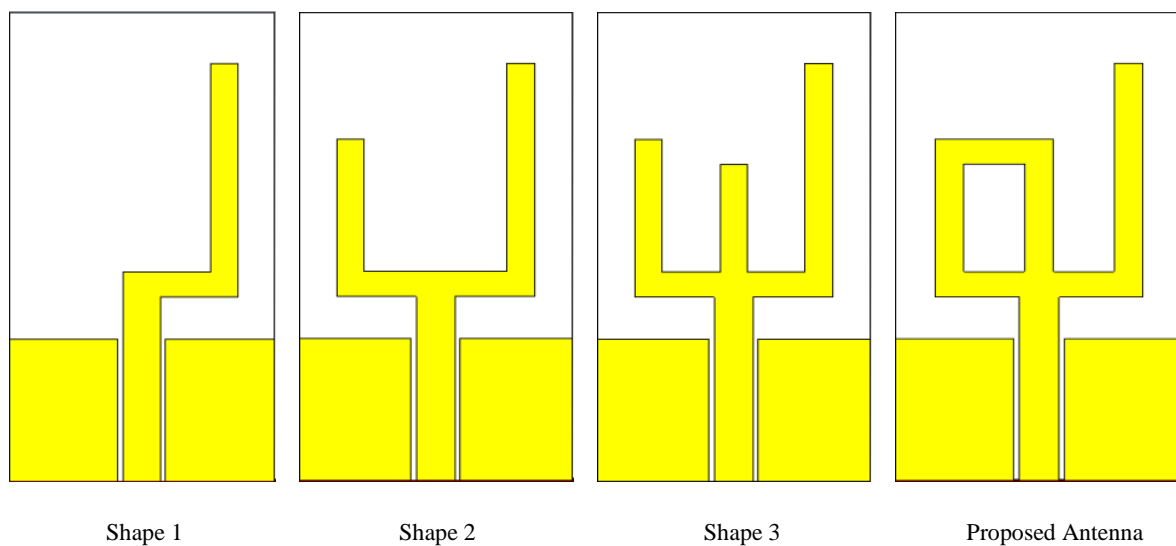


Fig. 2. Evolution of the proposed CPW-fed monopole antenna.

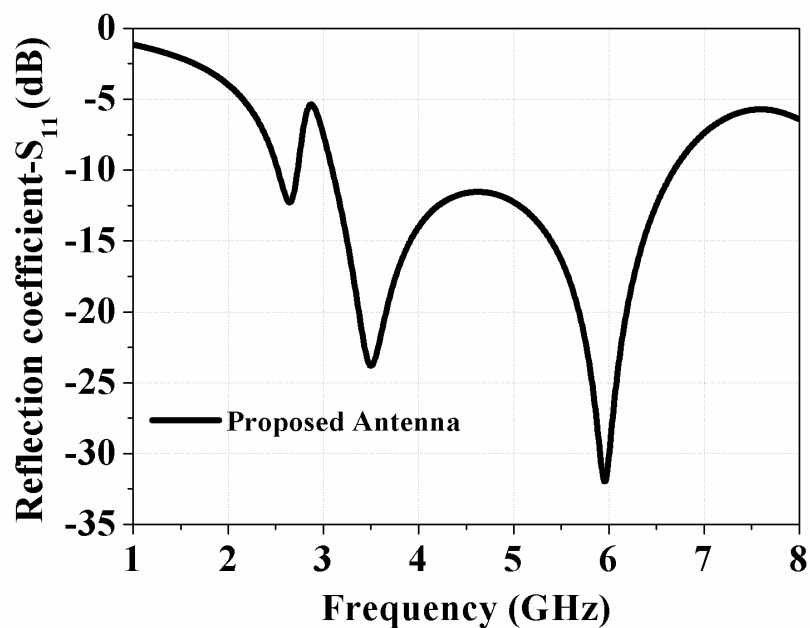


Fig. 3. Simulated result of the reflection coefficient against frequency for the proposed antenna.

Table II shows a comprehensive comparison antenna size among our proposed antenna and other compact multi-band antennas. As for our proposed antenna with an excellent dual-band characteristic and a smaller size than those of the previously proposed dual-band antennas.

TABLE II. COMPARISONS OF ANTENNA SIZE AMONG PROPOSED ANTENNA AND OTHER COMPACT ANTENNAS

Number	Published literature Reference	Size	Operating frequency band	$\frac{\text{Size proposed antenna}}{\text{Size reference antenna}} (\%)$
1	Peng and Ruan [2]	30×40 mm ²	2.50-2.75 GHz and 4.60-6.05 GHz	61.66
2	Peng and Ruan [4]	28×38 mm ²	2.25-2.65 GHz and 4.99-5.91 GHz	69.54
3	Pan et al. [6]	48×58 mm ²	2.01-4.27 GHz and 5.06-6.79 GHz	26.60
4	Chu and Ye [8]	28×33 mm ²	2.24-2.81GHz and 3.35-6.51 GHz	80.08
5	Karli and Ammor [19]	60×70 mm ²	2.72-2.76 GHz and 6.62-7.5 GHz	17.61
6	Tsai [20]	50×50 mm ²	1.90-2.75 GHz and 3.65-6.75 GHz	29.60
7	Xie et al [21]	40×40 mm ²	3.15-3.70 GHz and 5.05-5.97 GHz	46.25
8	Sim et al. [22]	30×45 mm ²	2.140-2.750 GHz and 5.05-6.16 GHz	54.81
9	Wu et al. [23]	75×75 mm ²	2.410-2.785 GHz and 4.575-6.355 GHz	13.15

III. PARAMETRIC STUDY

The parametric study is important for a design because it provides some understanding of the antenna characteristics to the antenna designer. Therefore, the effects of the design parameters for L_1 , L_2 , L_3 , (L_2 and L_3), W_1 and L_g on the initial antenna and the proposed monopole antenna characteristics are investigated here. The study is based on the antennas structures shown in Fig. 1.

A. The inverted L-shaped Stub1 (L_1)

The effects of the length L_1 of the initial antenna are plotted in Fig. 4(a). This figure shows the simulated reflection coefficient when the length of L_1 changes ($L_2= 10.5$ mm and $L_3= 8.5$ mm). By adjusting the length of L_1 , the total length of Stub1 varies. It is seen that the increase in L_1 decreases the resonant frequency of the first band and vice versa. The resonant frequency of the third band is also affected.

Fig. 4(b) shows the variation of the reflection coefficient of the proposed antenna when the length of the first Stub L_1 changed from 15.5 mm to 18.5 mm.

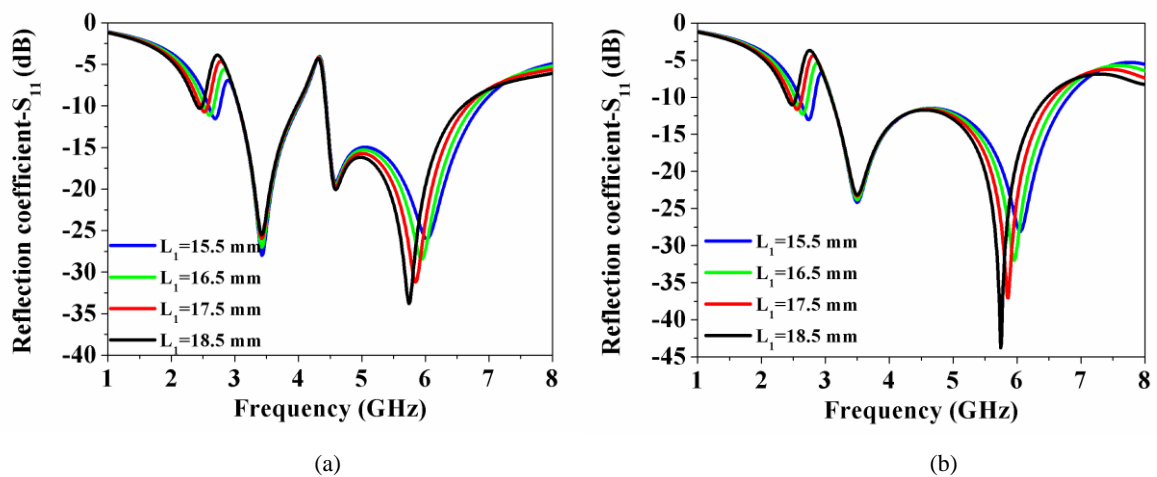


Fig. 4. Simulated reflection coefficients for different values of: (a) L_1 of the initial antenna and (b) L_1 of the proposed antenna.

B. The L-shaped Stub2 (L_2) of the initial antenna

Fig. 5(a) shows the simulation of the reflection coefficient with variation of L_2 ($L_1= 16.5$ mm and $L_3= 8.5$ mm) of the antenna presented in Fig. 1(a). By tuning the length of L_2 from 9.5 mm to 12.5 mm, it is clear that the raise in L_2 decreases the resonant frequency of the second band. The resonant frequency of the first band is slightly affected.

C. The rectangle Stub3 (L_3) of the initial antenna

Varying the length L_3 of the initial antenna to be 7.5, 8.5, 9.5 and 10.5 mm, it can be seen from Fig. 5(b) and Table III that with the increasing of length L_3 , the third resonant frequency shifts towards the lower frequency with an increase in the third band slightly, while the other resonant frequencies bands have not been changed.

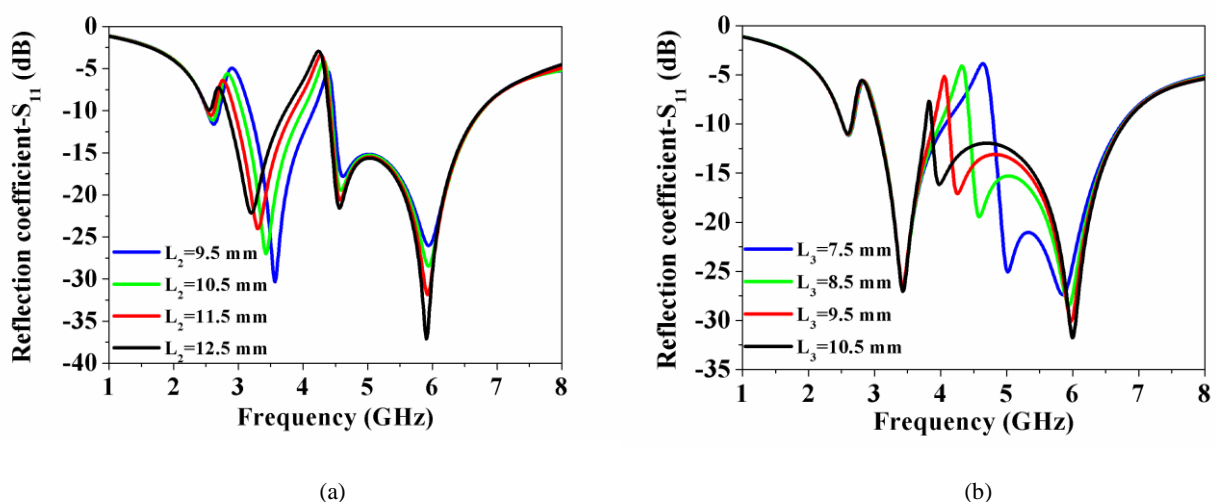


Fig. 5. Simulated reflection coefficients for different values of: (a) L_2 of the initial antenna and (b) L_3 of the initial antenna.

TABLE III. THE VALUES OF BANDWIDTH OF THE THIRD BAND FOR DIFFERENT VALUES OF L_3 OF THE INITIAL ANTENNA

Length L_3 (mm)	Third Band (GHz)
7.5	4.794-6.754 (1.940 GHz)
8.5	4.437-6.768 (2.331 GHz)
9.5	4.129-6.775 (2.646 GHz)
10.5	3.870-6.789 (2.919 GHz)

D. The simultaneous variation of L_2 and L_3 of the proposed antenna

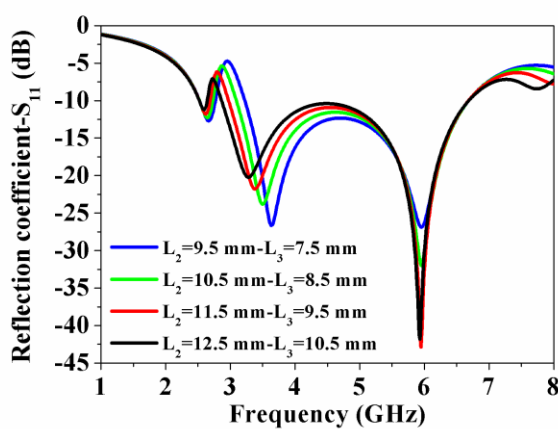
Fig. 6(a) shows the simulated reflection coefficient as a function of L_2 , the length of Stub2 and L_3 , the length of Stub3 of the proposed monopole antenna presented in Fig. 1(b). Small effects on the antenna's first and third resonant frequencies and large effects on the second resonant frequency are seen. The second band is shifted to lower frequencies with an increase in L_2 and the parameter S_{11} of the third resonant frequency is ameliorated when raising the length L_3 .

E. The width W_1 of the proposed antenna

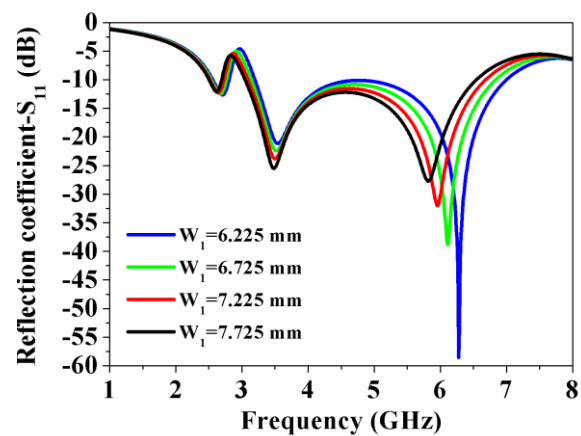
Fig. 6(b) shows the simulated reflection coefficient as a function of W_1 . It is seen from the plot that the 5-GHz operating band is strongly affected by the variations in W_1 , and the resonant frequency is shifted to lower frequencies when W_1 is increased from 6.225 mm to 7.725 mm and the level of S_{11} -parameter is enhanced from -27.70 dB to -58.57 dB. Small effects on the antenna's first and middle bands are also seen from the plot.

F. The effect of ground plane length L_g of the proposed antenna

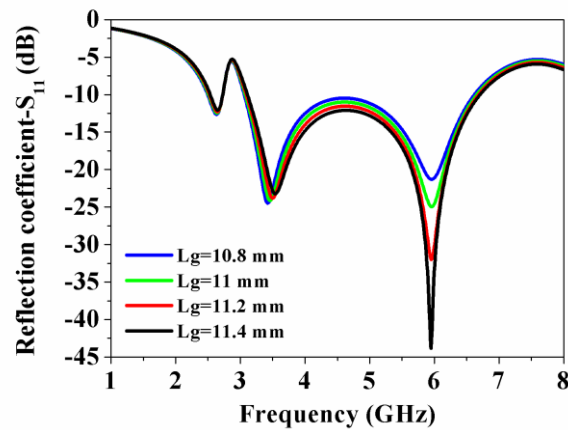
The finite ground CPW feeding mechanism of the proposed antenna is the capability of impedance matching at the operating frequencies. For this, the effect of the ground plane length L_g on the antenna characteristics has been illustrated. The effect of ground plane length L_g on the impedance matching is investigated and the reflection coefficient for the proposed antenna is shown in Fig. 6(c). It is observed that higher value of L_g gives a good impedance matching in the 5-GHz band.



(a)



(b)



(c)

Fig. 6. Simulated reflection coefficients for different values of: (a) L_2 and L_3 of the proposed antenna (b) W_1 of the proposed antenna and (c) L_g of the proposed antenna.

IV. RESULTS AND DISCUSSION

A. Reflection coefficient results

The dual-band planar monopole antenna is simulated using the CST Microwave Studio V13. A prototype structure of the proposed antenna has been constructed and experimentally studied. The SMA female connector is used for feeding with characteristic impedance of 50Ω , as shown in Fig. 7. The reflection coefficient is measured with Rohde and Schwarz ZVB 20 vector network analyzer, which its frequency range is, limited to 20 GHz. Fig. 8 shows the simulated and measured results of the reflection coefficient of the proposed antenna. The measured impedance bandwidths for $S_{11} \leq -10$ dB are about 110 MHz (2.62 to 2.73 GHz, $f_{r1} = 2.69$ GHz) and 4280 MHz (3.02 to 7.30 GHz, $f_{r2} = 4.28$ GHz and $f_{r3} = 6.86$ GHz), which makes it easy to cover the required bandwidths for WiMAX bands (3.40-3.69 GHz and 5.25-5.85 GHz), WLAN bands (5.15-5.35 GHz and 5.725-5.825 GHz) and a part of 2.60 GHz band from 2.50 to 2.69 GHz. Seen from Fig. 8, the simulated -10 dB impedance bandwidths for the first band is ranged from 2.519 to 2.729 GHz (210 MHz) and for the second band is ranged from 3.093 to 6.684 GHz (3591 MHz). We note a good agreement between the simulated and measured results with a good impedance matching in the operating bands. The small difference between the measured and simulated results is due to the effect of SMA connector soldering and fabrication tolerance.



Fig. 7. Photograph of the fabricated antenna.

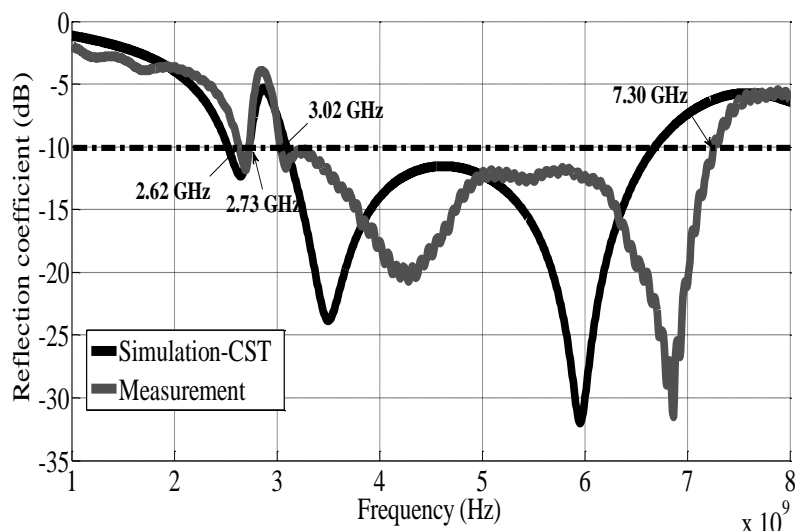


Fig. 8. The simulated and the measured reflection coefficient for the proposed antenna.

B. Current distributions of the initial antenna

From the simulated reflection coefficient characteristics of the initial antenna presented in Fig. 1(a), resonances can be observed at $f_1= 2.603$ GHz, $f_2= 3.429$ GHz and $f_3= 4.584$ GHz. The probable current paths for the first, the second and the third resonance frequencies are similar to resonant Path 1, resonant Path 2 and resonant Path 3, respectively, as shown in Fig. 1(a) (red line).

In order to better understand the initial antenna behavior, the current distributions of the three-band antenna at frequencies of 2.603 GHz, 3.429 GHz and 4.584 GHz are simulated and shown respectively in Figs. 9(a), (b) and (c). It can be evidently seen from Fig. 9 that the current distributions at the three resonant frequencies are different. Concerning the first resonant mode ($f_1= 2.603$ GHz), a large surface of the current density is observed along the inverted L-shaped Stub1. Whereas for the second frequency band ($f_2= 3.429$ GHz), the current distributions is mainly distributed along the L-shaped Stub2, on the other hand for the third resonant mode ($f_3= 4.584$ GHz), the current distributions becomes more concentrated along the Stub3. Nevertheless, they also have a common characteristic that is a large current is concentrated along the feed line.

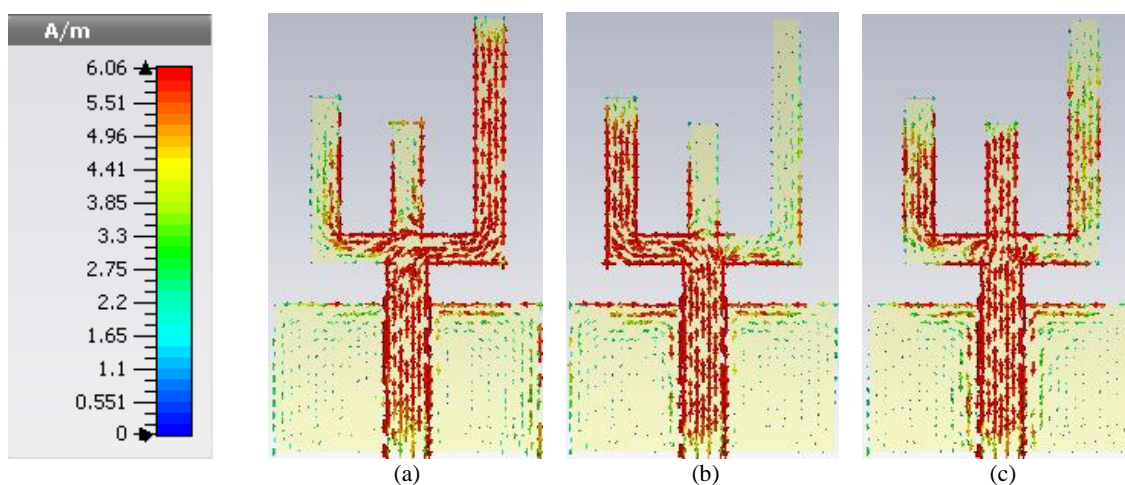


Fig. 9. Simulated current distribution of the initial antenna at frequencies (a) 2.603 GHz, (b) 3.429 GHz and (c) 4.584 GHz.

C. Current distributions of the proposed antenna

In order to further demonstrate the dual-band operation mechanism, the surface current distributions on the whole proposed antenna at different resonant frequencies are shown in Figs 10(a)-(c). It can be evidently seen that the current has different distributions along the optimized structure in different bands. Fig. 10(a) shows that the current distributions are forced to flow around the inverted L-shaped Stub1 and the rectangle Stub3. The variations on the length L_1 affect the second resonant frequency of the wide band. Figs 10(b) and 10(c) show the current distributions at frequencies 3.50 GHz and 4.60 GHz. The L-shaped Stub2 and the rectangle Stub3 contributed essentially to radiation at frequencies of 3.50 GHz and 4.60 GHz, respectively. The resonant currents at frequencies of 3.50 GHz and 4.60 GHz are distributed on both the Stub2 (L_2) and Stub3 (L_3).

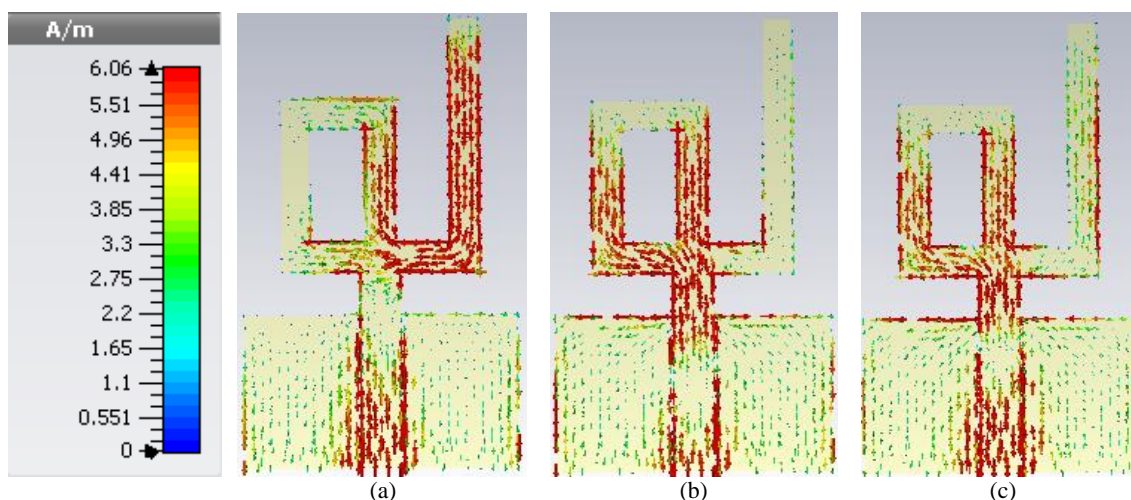


Fig. 10. Simulated current distribution of the proposed antenna at frequencies (a) 2.65 GHz, (b) 3.50 GHz and (c) 4.60 GHz.

D. Radiation patterns, gain and efficiency

The Simulated E-plane (YOZ) and H-plane (XOZ) radiation patterns at 2.65, 3.50, 5.20 and 5.80 GHz are normalized and shown in Fig. 11. It is observed that the proposed antenna has almost an omni-directional radiation patterns in the H-plane and nearly bi-directional radiation patterns in the E-plane over the desired operating bands.

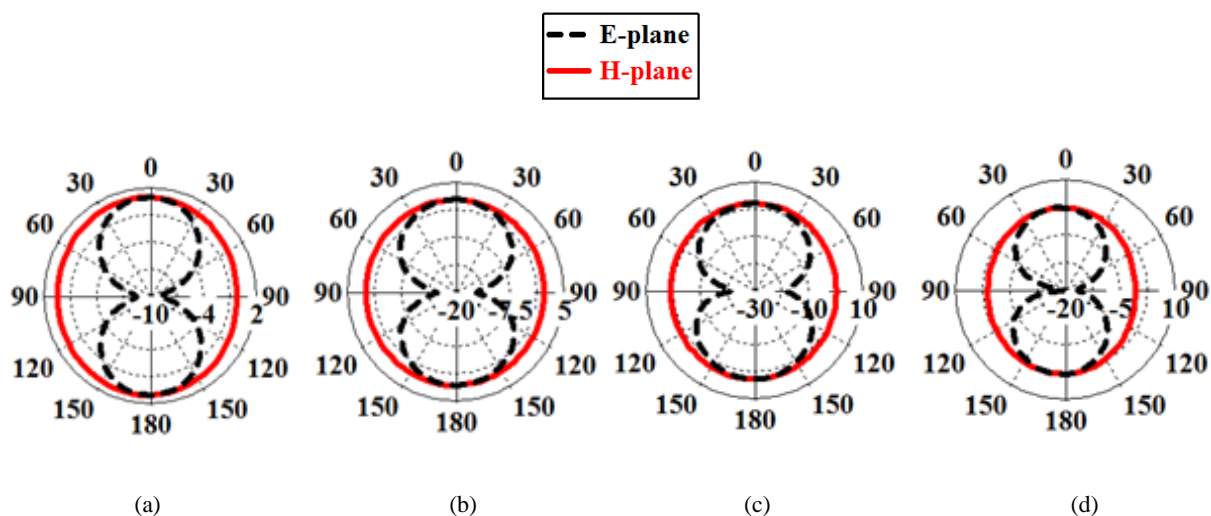


Fig. 11. Simulated 2D radiation patterns of the proposed antenna at frequencies (a) 2.65 GHz, (b) 3.50 GHz, (c) 5.20 GHz and (d) 5.80 GHz.

Fig. 12(a) and Fig. 12(b) show simulated peak gain and radiation efficiency across the operating bands. The maximum simulated peak antenna gains and radiation efficiencies are 1.45/1.55/3.31dBi and 81.1/77.5/75% at the first band and the second band, respectively.

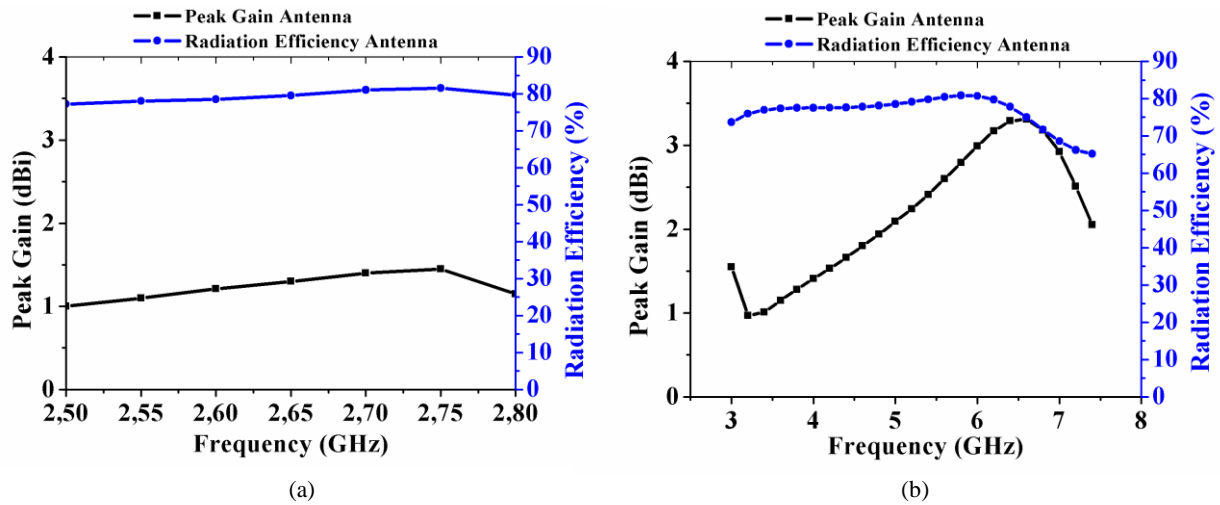


Fig. 12. Simulated peak gain and radiation efficiency across operating frequencies for proposed monopole antenna (a) first band, (b) second band.

V. CONCLUSION

A small monopole antenna for dual-band operations has been presented. The proposed monopole antenna has a simple planar structure and is easy to be printed on FR4 substrate with small size of $20 \times 37 \text{ mm}^2$. The initial antenna consists by three Stubs: inverted L-shaped Stub1, L-shaped Stub2 and rectangle Stub3. This configuration can generate three bands centered at about 2.603 GHz, 3.429 GHz and 4.584 GHz. The three resonant frequencies can be tuned individually by adjusting the length of the three Stubs. Thus, by combining between Stub2 and Stub3 (proposed antenna), two operating bands can be obtained with a wide second band which covers all the WiMAX bands 3.5/5.5 GHz and WLAN bands 5.2/5.8 GHz. Both the simulated and measured results show that the demonstrated antenna can successfully achieved two operating bands. The measured -10 dB reflection coefficient bandwidths cover 2.62-2.73 GHz (110 MHz) and 3.02-7.30 GHz (4280 MHz) bands, which satisfied the frequency requirements of WiMAX, WLAN and a part of the 2.6 GHz band from 2.50 to 2.69 GHz. In addition, the proposed antenna provides good radiation patterns in the working bands, which makes it suitable for integrating into portable devices. This CPW-fed planar monopole antenna is a good candidate for wireless communication systems.

ACKNOWLEDGMENT

This work was supported by the National Center for Scientific and Technical Research (CNRST). The authors would like to thank Professor Naima Amar Touhami from Faculty of Sciences of Tetouan for its beneficial and professional help in the realization of the proposed antenna.

REFERENCES

- [1] S. Jo, H. Choi, B. Shin, S. Oh, and J. Lee, "A CPW-Fed Rectangular Ring Monopole Antenna for WLAN Applications," *International Journal of Antennas and Propagation*, vol. 2014, Article ID 951968, 2014.
- [2] L. Peng, and C.-Li Ruan, "A Microstrip Fed Patch Antenna with Two Parasitic Invert L Stubs for Dual-Band WLAN Applications," *Wirel. Pers. Commun.*, vol. 57, no. 4, pp. 727-734, 2011.
- [3] L. Zhang, Y.-C. Jiao, G. Zhao, Y. Song, and F.-S. Zhang, "Broadband Dual-Band CPW-Fed Closed Rectangular Ring Monopole Antenna with a Vertical Strip for WLAN Operation," *Microwave and Optical Technology Letters*, vol. 50, no. 7, pp. 1929-1931, 2008.
- [4] L. Peng, and C.-L. Ruan, "A Microstrip Fed Monopole Patch Antenna with three Stubs for Dual-band WLAN Applications," *J. of Electromagn. Waves and Appl.*, vol. 21, no. 15, pp. 2359-2369, 2007.
- [5] C.-Y. Huang, and E.-Z. Yu, "A Slot-Monopole Antenna for Dual-Band WLAN Applications," *IEEE Antennas Wirel. Propag. Lett.*, vol. 10, pp. 500-502, 2011.
- [6] C.-Y. Pan, T.-S. Horng, W.-S. Chen, and C.-H. Huang, "Dual Wideband Printed Monopole Antenna for WLAN/WiMAX Applications," *IEEE Antennas Wirel. Propag. Lett.*, vol. 6, pp. 149-151, 2007.
- [7] J. Il Kim, and Y. Jee, "Design of Ultra wideband Coplanar Waveguide-Fed LI-Shape Planar Monopole Antennas," *IEEE Antennas Wirel. Propag. Lett.*, vol. 6, pp. 383-387, 2007.
- [8] Q.-X. Chu, and L.-H. Ye, "Design of Compact Dual-Wideband Antenna with Assembled Monopoles," *IEEE Trans. Antennas Propag.*, vol. 58, no. 12, pp. 4063-4066, Dec. 2010.
- [9] S. T. Fan, Y. Z. Yin, W. Hu, K. Song, and B. Li, "Novel CPW-Fed Printed Monopole Antenna with an n-Shaped Slot for Dual-Band Operations," *Microwave and Optical Technology Letters*, vol. 54, no. 1, pp. 240-242, 2012.
- [10] C.-M. Wu, J.-W. Syu, and W.-C. Liu, "Dual-Band Slotted Patch Antenna with Defective Ground for WLAN/WiMAX Applications," *Progress In Electromagnetics Research Letters*, vol. 53, pp. 1-6, 2015.
- [11] W. C. Liu, and W. R. Chen, "CPW-fed compact meandered patch antenna for dual-band operation," *Electronics Letters*, vol. 40, no. 18, pp. 1094-1095, 2004.
- [12] H.-D. Chen, and H.-T. Chen, "A CPW-Fed Dual-Frequency Monopole Antenna," *IEEE Trans. Antennas Propag.*, vol. 52, no. 4, pp. 978-982, 2004.
- [13] W. Hu, Y.-Z. Yin, P. Fei, and X. Yang, "Compact Triband Square-Slot Antenna with Symmetrical L-Strips for WLAN/WiMAX Applications," *IEEE Antennas Wirel. Propag. Lett.*, vol. 10, pp. 462-465, 2011.
- [14] A. Boutejdar, A. A. Ibrahim, and E. P. Burte, "A Compact Multiple Band-Notched Planer Antenna with Enhanced Bandwidth Using Parasitic Strip Lumped Capacitors and DGS-Technique," *TELKOMNIKA Indonesian Journal of Electrical Engineering*, vol. 13, no. 2, pp. 203-208, 2015.
- [15] A. Boutejdar, A. A. Ibrahim, and E. P. Burte, "Novel Microstrip Antenna Aims at UWB Applications," *Microwaves & RF*, vol. 7, no. 7, pp. 8-14, 2015.
- [16] A. A. Ibrahim, M. A. Abdalla, and A. Boutejdar, "Resonator Switching Techniques for Notched UWB Antenna in Wireless Applications," *IET Microwaves, Antennas & Propagation*, vol. 9, no. 13, pp. 1468-1477, 2015.
- [17] A.A. Ibrahim, M.A. Abdalla, and A. Boutejdar, "A Printed Compact Band Notched Antenna Using Octagonal Radiating Patch and Meander Slot Technique for UWB Applications," *Progress In Electromagnetics Research M*, vol. 54, pp. 153-162, 2017.
- [18] A. Boutejdar, and W. Abd Ellatif, "A novel compact UWB monopole antenna with enhanced bandwidth using triangular defected microstrip structure and stepped cut technique," *Microwave and Optical Technology Letters*, vol. 58, no. 6, pp. 1514-1519, 2016.
- [19] R. Karli, and H. Ammor, "Rectangular patch antenna for dual-band RFID and WLAN applications," *Wirel. Pers. Commun.*, vol. 83, no. 2, pp. 995-1007, 2015.
- [20] Lin C. Tsai, "Design of Triple-Band T-U-Shaped CPW-Fed Slot Antennas," *Microwave and Optical Technology Letters*, vol. 56, no. 4, pp. 844-848, 2014.

- [21] J.-J. Xie, X.-S. Ren, Y.-Z. Yin, and S.-L. Zuo, "Rhombic Slot Antenna Design with a Pair of Straight Strips and Two n-Shaped Slots for WLAN/WiMAX Applications," *Microwave and Optical Technology Letters*, vol. 54, no. 6, pp. 1466-1469, 2012.
- [22] C.-Y.-Desmond Sim, Y.-W. Hsu, and C.-H. Chao, "Dual Broadband Slot Antenna Design for WLAN Applications," *Microwave and Optical Technology Letters*, vol. 56, no. 4, pp. 983-988, 2014.
- [23] J.-W. Wu, H.-M. Hsiao, J.-H. Lu, and S.-H. Chang, "Dual broadband design of rectangular slot antenna for 2.4 and 5 GHz wireless communication," *Electronics Letters*, vol. 40, no. 23, pp. 1461-1463, 2004.